

Article

Design and Testing of the Double-Symmetric Eccentric Exciter for Fruit Tree Vibration Harvest

Haobo Jiao ¹ , Juming Luo ¹, Aifei Tang ¹, Lihong Wang ¹, Chen Ma ¹, Yaping Li ² and Chongsong Li ^{1,3,*}

¹ College of Engineering and Technology, Southwest University, Chongqing 400715, China; jiaohaobo@swu.edu.cn (H.J.); luo_juming@163.com (J.L.); 19566187382@163.com (A.T.); wlh_shz@163.com (L.W.); marcia.chen@foxmail.com (C.M.)

² College of Mechanical and Electrical Engineering, Shihezi University, Shihezi 832000, China; lyp_shz@163.com

³ Key Laboratory of Agricultural Equipment in Hilly and Mountainous Areas, Chongqing 400715, China

* Correspondence: l20190304@swu.edu.cn; Tel./Fax: +86-153-3450-1020

Abstract: The amplitude of excitation force from exciters used in fruit tree vibration harvesting remains constant at a given frequency, leading to poor fruit detachment ratio and tree damage. A solution has been proposed through the development of a Double-Symmetric Eccentric Exciter (DSEE). This new exciter allows for the adjustment of excitation force amplitude while maintaining a constant frequency by varying the phase angle of the DSEE. To validate the effectiveness of the DSEE, vibration tests were conducted on fruit trees using different parameter exciting forces. Acceleration sensors were employed to measure the vibration accelerations of the tree branches. The experimental results revealed that when a fixed frequency excitation force with a constant phase angle was applied to the trunk, the vibration acceleration of branches exhibited inconsistent variations due to differences in the vibration differential equation parameters of each branch. Furthermore, it was observed that increasing the phase angle of the DSEE at a fixed frequency led to larger vibration accelerations in every branch. This signifies that adjusting the phase angle of the DSEE can effectively increase the amplitude of the exciting force. Consequently, the ability to control both the amplitude and frequency of the excitation force independently can mitigate issues such as low fruit harvest rates and minimize damage to fruit trees.

Keywords: fruit trees; DSEE; eccentric block; acceleration; vibration



Citation: Jiao, H.; Luo, J.; Tang, A.; Wang, L.; Ma, C.; Li, Y.; Li, C. Design and Testing of the Double-Symmetric Eccentric Exciter for Fruit Tree Vibration Harvest. *Agriculture* **2024**, *14*, 570. <https://doi.org/10.3390/agriculture14040570>

Academic Editor: Dainius Steponavičius

Received: 14 January 2024

Revised: 17 March 2024

Accepted: 21 March 2024

Published: 2 April 2024



Copyright: © 2024 by the authors. Licensee MDPI, Basel, Switzerland. This article is an open access article distributed under the terms and conditions of the Creative Commons Attribution (CC BY) license (<https://creativecommons.org/licenses/by/4.0/>).

1. Introduction

Fruits and nuts are rich in medicinal ingredients [1–4]. In addition, fruits and nuts are rich in vitamins and other nutrients that people need every day. The demands for these constituents promote the vigorous development of the forest fruit planting and harvesting. With the development of fruit harvesting technology, trunk vibration harvesting technology has become more widely used for many kinds of fruit trees [5,6]. Fruit tree harvesting technologies, especially trunk vibration harvesting techniques, have been widely applied for various types of fruit trees. This approach has not only improved efficiency but also ensured minimal damage to the fruit trees, thereby enhancing overall productivity and quality of the harvest.

To enhance the operational efficiency of vibratory harvesting machines, researchers have conducted extensive studies. In the research on parameter optimization of vibratory harvesting machinery, it was discovered that the frequency and amplitude of the excitation force, as well as the location of excitation on trunks, significantly impacted the performance of fruit tree vibration harvesting. The vibration frequency and amplitude are generated by the exciter utilized for fruit vibration harvesting, making the exciter a crucial component in fruit tree vibration harvesting [5–9].

At present, existing fruit tree exciters are driven by a single shaft or a double shaft. They can often be divided into four types: symmetric double eccentric exciters, single eccentric exciters, asymmetric double eccentric exciters, and orthogonal eccentric exciters [7–9]. The amplitudes of these exciters change with the exciting frequencies in a square relation. It is uncertain if this relationship aligns with the amplitude–frequency relationship required for fruit vibration harvesting. Existing shakers face a common issue where the amplitudes (F) of the exciting force vary with vibration frequency (f) according to $F = me(2\pi f)^2$, where m represents the quality of eccentric blocks, and e denotes the eccentric distance of the blocks. When the vibration frequency remains constant, the vibration amplitude cannot be altered.

A low amplitude of vibration force at a small exciting frequency may not generate sufficient vibration acceleration in the branches to make the fruits fall. Conversely, a high exciting frequency can lead to an excessively large exciting force on the trunks, potentially causing damage to the fruit trees. This phenomenon hinders the advancement of fruit harvesting technology [10–13]. This phenomenon hinders the advancement of fruit harvesting technology.

It has also been observed that the frequency of excitation impacts the rate at which fruits detach. A higher exciting frequency results in more efficient transfer of vibration energy from the exciter to the fruit, leading to a higher fruit detachment rate [14–17]. This seems like an apt statement; however, the amplitude of the exciting force is ignored. As the exciting frequency increases, the amplitude of the exciting force will also increase with the square of the exciting frequency. Therefore, the vibration energy exerted by the exciter on the fruit tree will be larger per unit time [15,18]. Therefore, it is necessary to analyze the influence of excitation amplitude and excitation frequency on the acceleration of the branches separately.

This paper analyzes the principle of existing exciters and proposes the DSEE. A vibration test was conducted on fruit trees, where different parameter exciting forces were applied to excite the trees, and the resulting vibration accelerations of branches were recorded. Due to the unique differential equations of the vibration of branches, the vibration accelerations varied among branches even under the same exciting force. Furthermore, the amplitude of the exciting force generated by the DSEE can be adjusted by manipulating the phase angle. This feature allows for the adjustment of exciting forces with the same frequency by altering the phase angle, potentially preventing issues like low fruit harvest rates and damage to fruit trees.

2. Materials and Methods

2.1. Existing Vibration Harvesting Exciters

The single eccentric exciter (Figure 1a) can only generate torsional vibration [18–20]. The direction of the exciting force angular (ωt) varies with time t , while the amplitude ($me\omega^2$) remains constant. In the symmetric double eccentric exciter (Figure 1b), the angular velocity directions of the two eccentric blocks are opposite, but their angular velocity magnitudes are the same. In the x-axis direction, the vector sum of the centrifugal forces produced by two eccentric blocks is 0. In the y-axis direction, the vector sum of the centrifugal forces produced is their algebraic sum. The symmetric double eccentric exciter produces a linear reciprocating vibration. The symmetric double eccentric exciter generates linear reciprocating vibration. In contrast, the asymmetric double eccentric block exciter (Figure 1c) differs from the two exciters mentioned earlier as its parameters (e_1 and e_2 , ω_1 and ω_2 , m_1 and m_2) are not the same, respectively. In addition, the orthogonal eccentric blocks (Figure 1d) can generate a tri-dimensional exciting force with its direction and magnitude changing according to the mass and rotation of the eccentric blocks [9]. The amplitudes of all exciters mentioned in Figure 1 change with vibration frequencies in the square relation, which is expressed as Equation (1).

$$F = 2me(2\pi f)^2 \sin(2\pi ft + \varphi) \quad (1)$$

where ω is rotation speed (vibration frequency, $f = \omega/2\pi$), rad/s; φ is phase angle, rad; m is mass, kg; and e is eccentric distance, m.

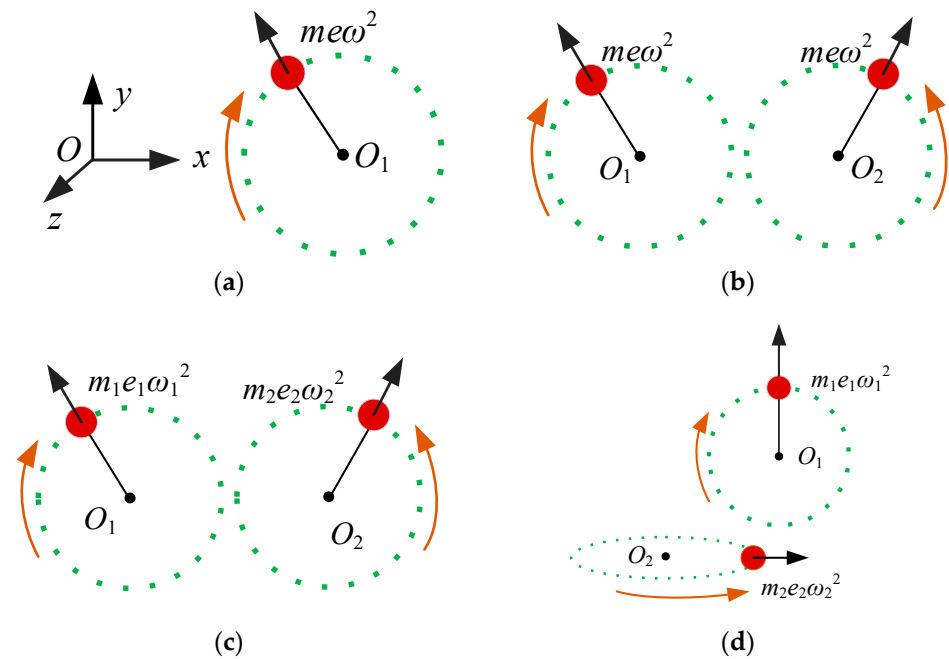


Figure 1. Mechanical model of 4 common exciter structures: (a) single eccentric exciter; (b) symmetrical double eccentric exciter; (c) asymmetric double eccentric exciter; and (d) orthogonal eccentric exciter. Note: m , m_1 , and m_2 are the masses of the eccentric blocks, kg; e is the eccentric distance, m; ω , ω_1 , and ω_2 are the angular rates of rotation of the eccentric blocks, rad/s; t is the time, s; and $me\omega^2$ is the centrifugal force of eccentric block, N.

The amplitude and frequency of the excitation force are related in fruit vibration harvesting. A higher excitation frequency is required for trees that need a larger amount of vibration acceleration to be produced by the branches. And the larger exciting frequencies can improve the energy transfer efficiency of fruit trees and fruit detachment rate. However, it can be observed from formula (1) that the amplitude of the excitation force will increase in a square relationship with the excitation frequency. Excessive excitation force can lead to damage in the clamping position and roots of fruit trees. These injuries can impact nutrient transport and reduce fruit yield. Conversely, some fruit trees have low vibration frequencies. The existing exciters with low excitation frequencies may not generate sufficient exciting force necessary for effective harvesting. As a result, the vibration acceleration of the branches is reduced, leading to some fruits not falling off and decreasing the overall fruit detachment rate. Hence, the frequency and amplitude of the excitation force are crucial factors in fruit tree vibration harvesting. Furthermore, the square relationship between frequency and amplitude of the excitation force significantly impacts the performance of fruit tree vibration harvesting.

For a single eccentric block, the centrifugal force generated during rotation is a physical law. And its magnitude with a certain angular velocity cannot be changed. Hence, the frequency and amplitude of the excitation force can only be regulated by the vector sum of centrifugal force generated by multiple eccentric blocks. The DSEE was developed to be used for fruit vibration harvesting and investigate the relationship between amplitude and frequency of excitation force in fruit vibration harvest.

For a single eccentric block, the centrifugal force generated during rotation follows a physical law, and its magnitude at a certain angular velocity remains constant. Therefore, the frequency and amplitude of the excitation force can only be adjusted by the vector sum of centrifugal forces generated by multiple eccentric blocks. The DSEE was developed

specifically for fruit vibration harvesting to study the correlation between the amplitude and frequency of the excitation force in fruit vibration harvesting.

2.2. Three-Dimensional Model of the DSEE

The DSEE is depicted in Figure 2. The operating principle of the DSEE is illustrated in Figure 2a, where the initial phases of the first pair of eccentric blocks are perpendicular to the x-axis, and the second pair of eccentric blocks have an x-axis angle of φ , known as the phase angle of the DSEE. The rotation speeds of the four eccentric blocks are equal, but the rotation directions of each pair of eccentric blocks are opposite. The excitation force of the DSEE is defined by Equation (2). The amplitude ($|F| = 2e\omega^2(m_1 + m_2\cos(\varphi))$) of the excitation force can be adjusted by the angle φ . Consequently, the DSEE enables the independent adjustment of the amplitude and frequency of the excitation force to better suit vibration harvesting needs. A three-dimensional model of the DSEE was created using SolidWorks as shown in Figure 2b. Each pair of eccentric blocks is interconnected by a gear pair.

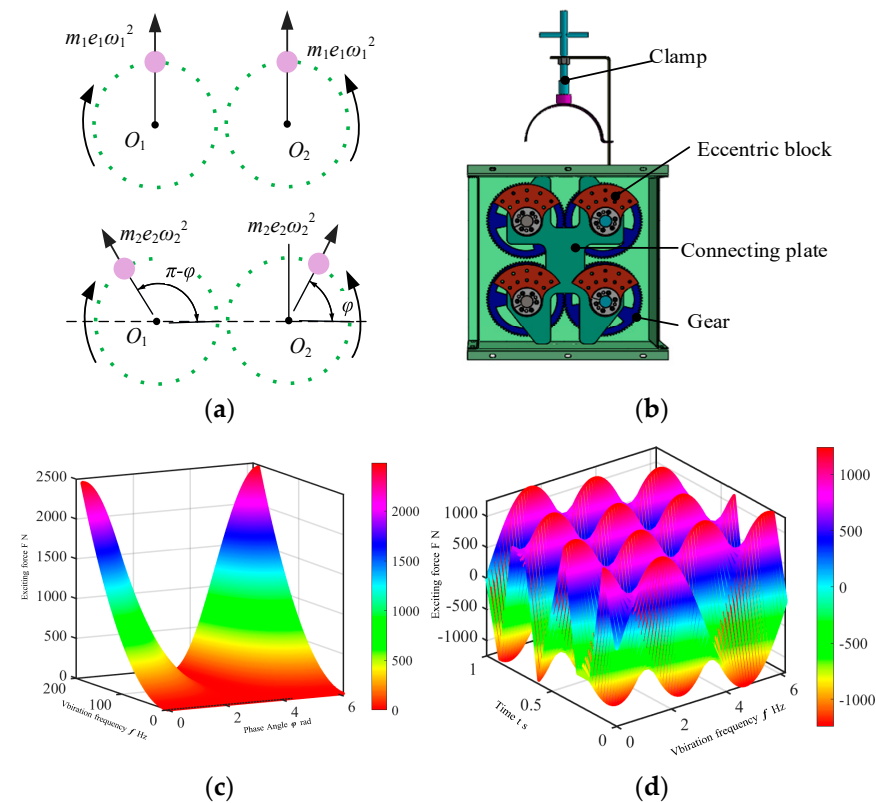


Figure 2. Design and amplitude–frequency relationship of the DSEE eccentric block: (a) principle of the DSEE eccentric block; (b) 3D structure of the DSEE eccentric block; (c) the variation law of the amplitude, phase angle, and vibration frequency; and (d) variation force F with the phase angle φ and the time t .

$$F(\omega, \varphi, t) = 2e\omega^2(m_1 + m_2 \cos(\varphi)) \sin(\omega t) \tag{2}$$

When the mass, rotation, and radius of the DSEE are constant, the relationship between the phase angle φ and vibration frequency f is illustrated in Figure 2c. At $\varphi = -0.5\pi$, the amplitude of the DSE blocks remains constant, with varying vibration frequencies reaching zero. Consequently, the DSEE does not exhibit any vibration phenomenon. With a constant vibration frequency, the amplitude increases from $-\pi/2$ to $\pi/2$ and from $-\pi/2$ to $-3/2\pi$. This variation is symmetric around the plane $\varphi = -\pi/2$. The adjustment range for the excitation force amplitude is selected within the φ range of $-\pi/2$ to $\pi/2$. Within

this interval, the amplitude of the excitation force increases as the phase angle φ rises, while maintaining a fixed excitation frequency. When the vibration frequency is fixed, the amplitude changes with the phase angle φ and time t , as depicted in Figure 2d. The amplitude of the DSEE follows a cosine law. At a specific phase angle φ , the amplitude of the DSEE oscillates sinusoidally over time t .

The amplitude of the DSEE is adjusted by the phase angle φ . For certain fruit trees with small trunks, low exciting frequencies are required due to the fundamental frequency of fruit trees being $\omega = (3Ed^2 / (16\rho l^3))^{0.5}$, where E represents the modulus of elasticity, d is the diameter of the trunk, ρ is the density of the fruit tree, and l is the length of the trunk. On the other hand, fruit trees with larger trunks may require higher optimal vibration frequencies. However, the acceleration needed for fruit detachment remains constant for any fruit tree. To minimize vibration damage caused by excessive excitatory force amplitudes to the fruit tree, adjusting the amplitude of the excitatory force is essential. In comparison to the exciters in Figure 1, the DSEE can modify the amplitude of the excitation force while maintaining a fixed excitation frequency, thereby enhancing the adaptability of the excitation force to various types of fruit trees.

2.3. Experimental Method of Amplitude–Frequency Requirement Test of Fruit Vibration Harvest

To investigate the DSEE’s capability to adjust the amplitude of the exciting force based on the phase angle φ , a fruit tree vibration test involving variable frequency and amplitude excitations was conducted, as illustrated in Figure 3. The hardware setup for the fruit tree shaking device, depicted in Figure 3a, included a Huawei MagicBook2019 computer (model VLR-W29L, made in Guangzhou of China), two servomotors (SDGA-08C11BD, made in Shenzhen of China), two adapter drivers (TSDA-C218, made in Shenzhen of China), a dual-symmetric eccentric block exciter, a tri-axis acceleration sensor (WT901SDCL, made in Shenzhen of China, mass of 2 g), and a DC power supply (made in Shantou of China). The DC power supply provided 48 V DC to the two servomotors. The computer was connected to the adapter driver via an RS232 serial port to regulate the speed and position of the two servomotors.

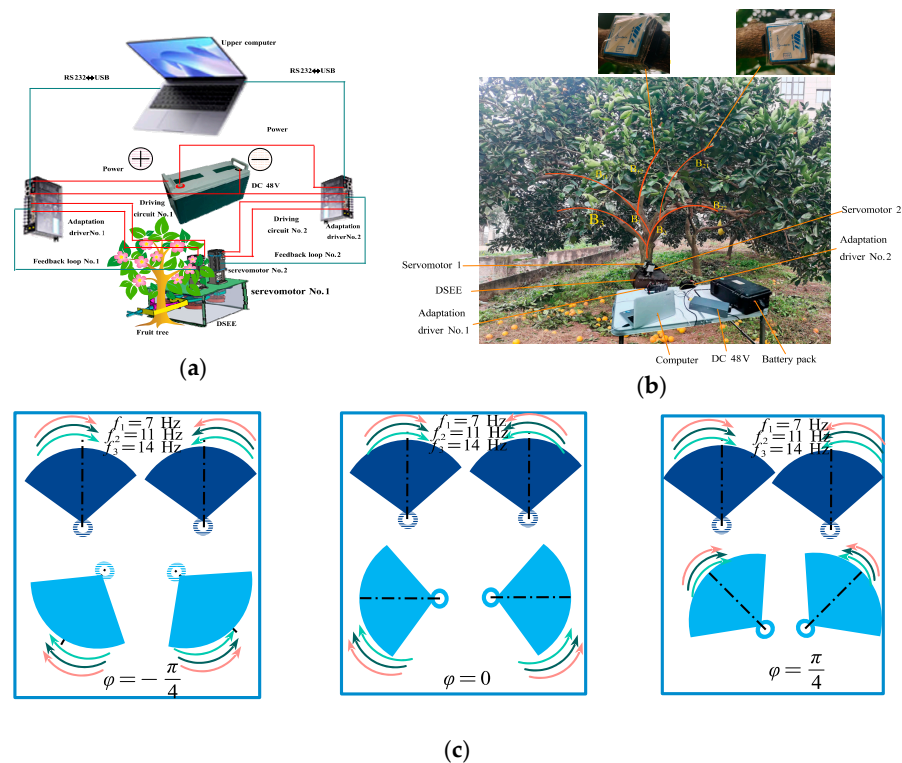


Figure 3. The amplitude–frequency test of fruit tree excitation force: (a) test device connection mode; (b) fruit tree vibration test; and (c) frequency and phase angle setting method.

The DSEE is mounted on the tree trunk, and the fruit tree is subjected to excitation from different exciter frequencies and phase angles. The phase angles φ of the DSEE are set as $-\pi/4$, 0 , $\pi/4$ successively, while the excitation frequencies are specified as 7 Hz, 11 Hz, and 14 Hz in Figure 3c. Vibration accelerations on the branches are gauged by two triaxial acceleration sensors (A_1 and A_2) in Figure 3b. The branches being measured have diameters ranging from 3.5 to 4.5 cm. These two acceleration sensors are situated approximately 40 cm from the ends of the branches, where numerous fruits grow. An analysis is carried out on the impact of the excitation force on branch acceleration at diverse excitation frequencies and phase angles. The agronomic parameters and primary structural details of the tested fruit tree are presented in Table 1. The citrus tree exhibits an open-heart tree shape.

Table 1. Test the main parameters of fruit trees.

Parameter Name	Value
Variety of fruit tree	Citrus tree
Spacing of tree rows/m	5.6
The bead spacing of citrus trees/m	4.8
Diameter of 60 cm high trunk/cm	11.2–14.8
Fruit tree height/m	3.6–4.2
Crown radius/m	2.2–2.6

During the fruit tree acceleration detection process, the negligible mass and volume of the acceleration sensor in comparison to the branch lead to the disregard of the sensor’s impact on branch vibration acceleration. Therefore, the vibration signal captured by the acceleration sensor is regarded as the true vibration acceleration signal of the branch. The outcomes of the tests are displayed in Figures 4 and 5.

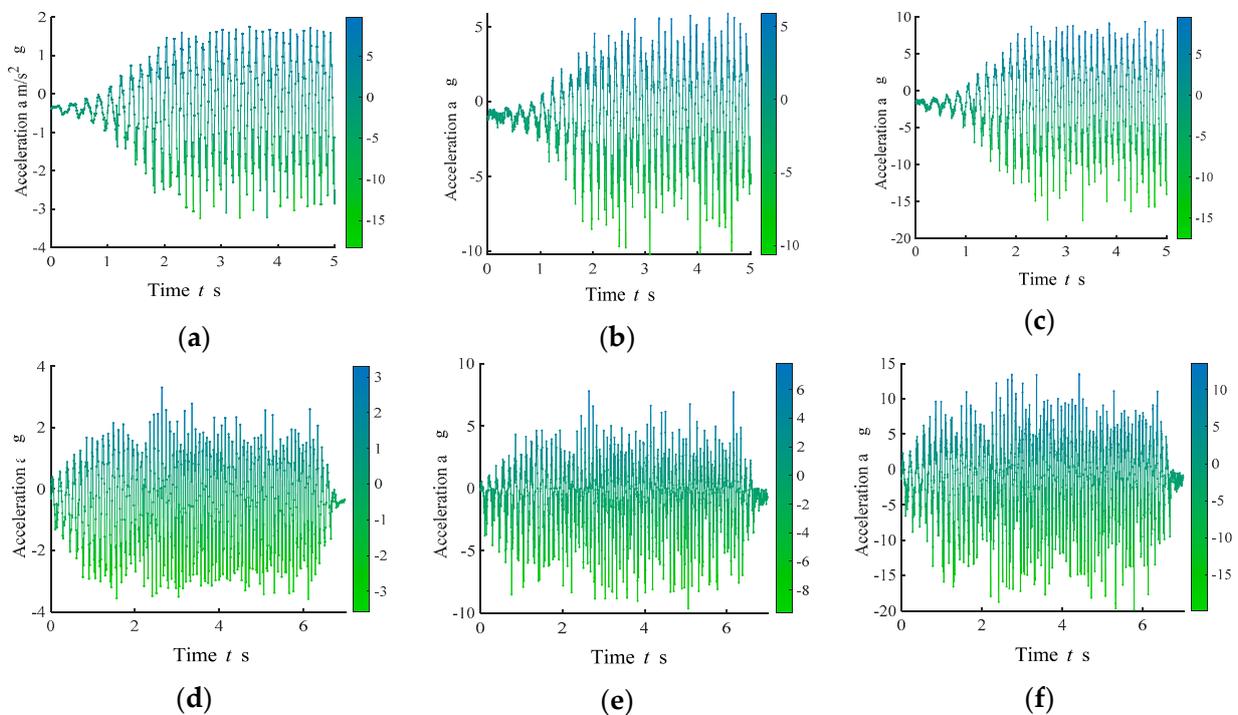


Figure 4. Cont.

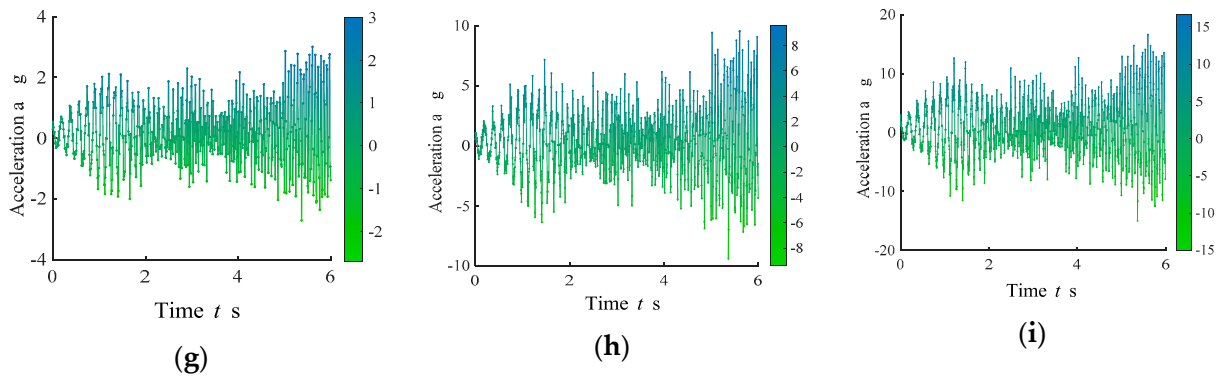


Figure 4. Vibration acceleration of B_{12} at excitation force with different parameters: (a) $f = 7$ Hz, $\varphi = -\pi/4$; (b) $f = 7$ Hz, $\varphi = 0$; (c) $f = 7$ Hz, $\varphi = \pi/4$; (d) $f = 11$ Hz, $\varphi = -\pi/4$; (e) $f = 11$ Hz, $\varphi = 0$; (f) $f = 11$ Hz, $\varphi = \pi/4$; (g) $f = 14$ Hz, $\varphi = -\pi/4$; (h) $f = 14$ Hz, $\varphi = 0$; and (i) $f = 14$ Hz, $\varphi = \pi/4$. Note: g represents the acceleration of gravity with a magnitude of 9.8 ms^{-2} .

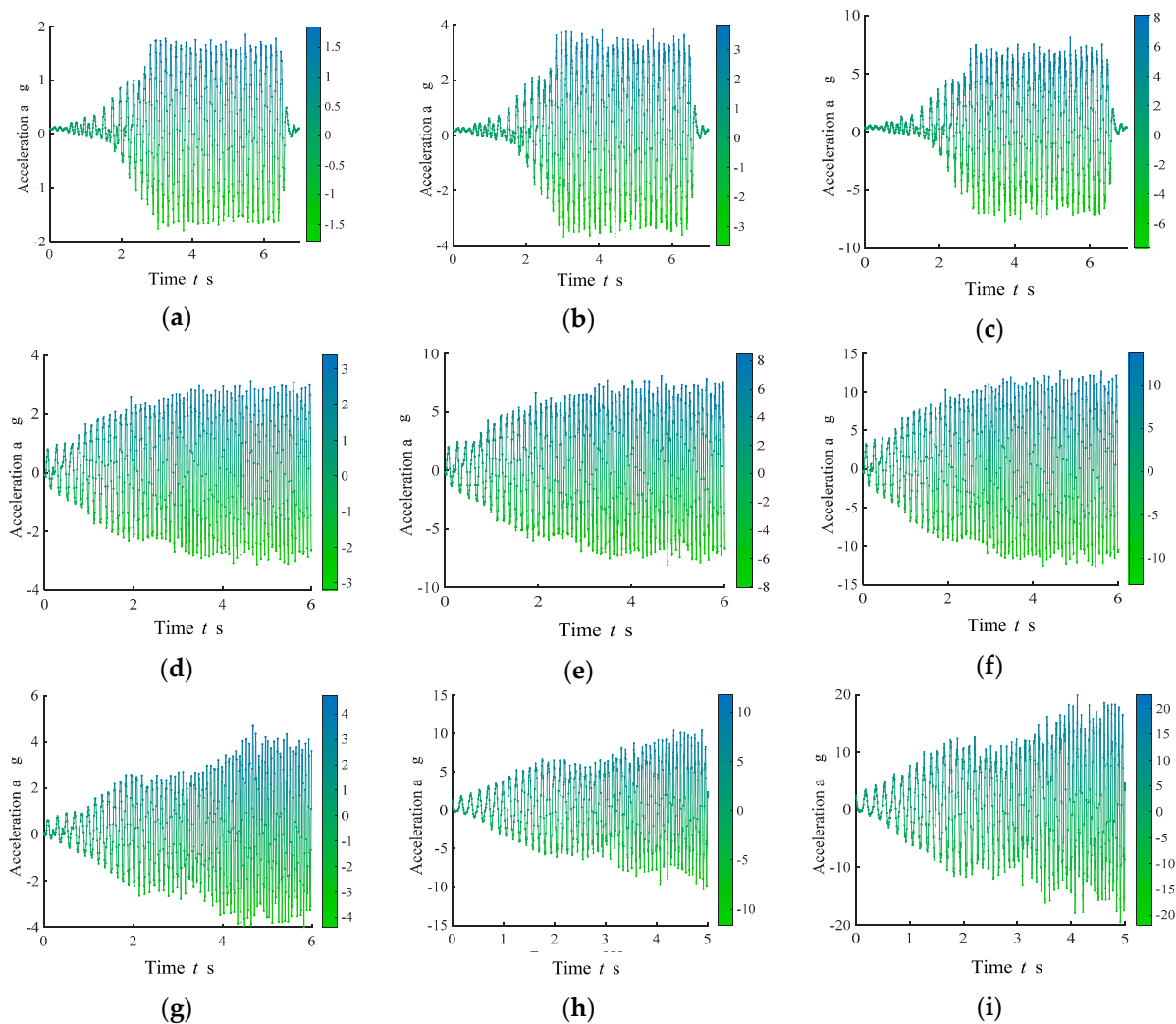


Figure 5. Vibration acceleration of B_{21} at excitation force with different parameters: (a) $f = 7$ Hz, $\varphi = -\pi/4$; (b) $f = 7$ Hz, $\varphi = 0$; (c) $f = 7$ Hz, $\varphi = \pi/4$; (d) $f = 11$ Hz, $\varphi = -\pi/4$; (e) $f = 11$ Hz, $\varphi = 0$; (f) $f = 11$ Hz, $\varphi = \pi/4$; (g) $f = 14$ Hz, $\varphi = -\pi/4$; (h) $f = 14$ Hz, $\varphi = 0$; and (i) $f = 14$ Hz, $\varphi = \pi/4$. Note: g represents the acceleration of gravity with a magnitude of 9.8 ms^{-2} .

3. Results

The vibration acceleration of branches B_{12} and B_{21} over time t is displayed in Figures 4 and 5. When excitation forces of the same frequency but varying amplitudes were applied to the trunk, the vibration accelerations of different branches exhibited distinct changing trends over time. When the excitation force of different exciting frequencies was applied to the trunk, the changing trends of vibration acceleration of the same branch were also different. When the excitation force of the same frequency was applied to the trunk and the phase angle φ of the DSEE was increased, the vibration accelerations of the branches showed an upward trend. Additionally, the trends of vibration accelerations for each branch were similar in nature.

In Figure 4, when the exciting force with the frequency of 7 Hz was applied to the trunk, the branch B_{12} was in steady state vibration, and the amplitude of acceleration vibration fluctuated very little. The vibration acceleration reaches its maximum amplitudes of 1.78 g, 4.89 g, and 7.96 g when the phase angles are $-\pi/4$, 0, and $\pi/4$ in Figure 4a–c. The amplitude of vibration acceleration fluctuates obviously under the exciting force with the frequency of 11 Hz applied to the trunk. The vibration acceleration reaches its maximum amplitudes of 2.21 g, 5.03 g, and 9.28 g when the phase angles are $-\pi/4$, 0, and $\pi/4$ in Figure 4d,f. The acceleration amplitude fluctuates greatly when the exciting force of the frequency of 14 Hz is applied to the trunk. The vibration acceleration reaches its maximum amplitudes of 2.32 g, 8.36 g, and 15.23 g when the phase angles are $-\pi/4$, 0, and $\pi/4$ in Figure 4g–i. Therefore, the amplitude of excitation force with fixed excitation frequency increases. In addition, the amplitude fluctuation of the accelerations in the branch B_{12} increases with the larger excitation frequency f .

In Figure 5, when the exciting force of a 7 Hz frequency was applied to the trunk, the amplitude of the vibration acceleration of branch B_{21} showed minimal fluctuation. The vibration acceleration reaches its maximum amplitudes of 1.85 g, 3.92 g, and 6.63 g when the phase angles are $-\pi/4$, 0, and $\pi/4$ in Figure 5a–c. With an exciting force of 11 Hz frequency applied to the trunk, there was a slight fluctuation in the amplitude of vibration acceleration. The vibration acceleration reaches its maximum amplitudes of 2.62 g, 5.86 g, and 11.28 g when the phase angles are $-\pi/4$, 0, and $\pi/4$ in Figure 5d–f. Under the exciting force of a 14 Hz frequency applied to the trunk, the amplitude of vibration acceleration in branch B_{21} increased over time. The vibration acceleration reaches its maximum amplitudes of 3.92 g, 9.86 g, and 17.28 g when the phase angles are $-\pi/4$, 0, and $\pi/4$ in Figure 5g–i.

To analyze the feasibility of adjusting the scheme of fruit tree vibration more accurately by changing the amplitude of the exciting force via adjusting the phase angle φ , we calculated the absolute value of the branch vibration acceleration a_i and determined its average value a_v using Equation (3). By adjusting the phase angle φ , the vibration acceleration of branches a_v can be modified. This approach provides a more comprehensive method to confirm the adjustability of the excitation force amplitude. The results are illustrated in Figure 6.

$$\alpha_v = \sum_{i=1}^N \frac{|\alpha_i|}{N} \quad (3)$$

where N represents the number of samples collected by the acceleration sensor, and a_i represents the acceleration value of each sample point.

In Figure 6a, when the frequency of the exciting force remains constant, the average acceleration a_v of B_{12} increases with the larger amplitude of the exciting force. However, when the phase angle is constant, the vibration acceleration of B_{12} has no obvious change trend with the increase in excitation force frequency. In Figure 6b, average vibration acceleration a_v of B_{21} shows an increasing trend with the larger exciting frequency f .

The analysis of the test results reveals inconsistencies in the acceleration of branches under varying excitation force parameters. As the excitation force amplitude increases, the acceleration of the branches demonstrates a rising trend. However, the average accelera-

tion a_v of different branches does not exhibit consistency with the increase in excitation force frequency.

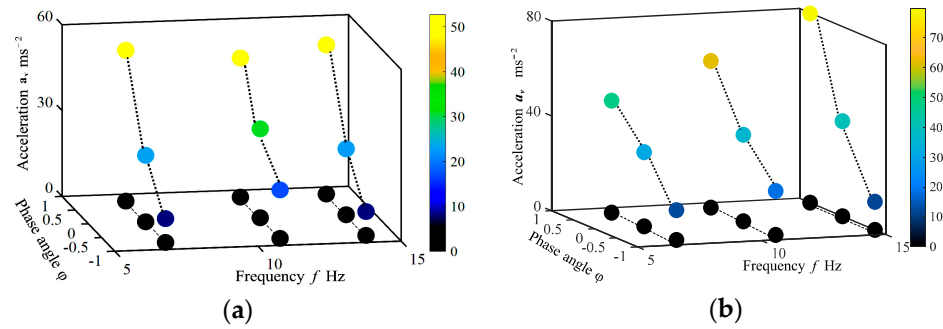


Figure 6. Variation in the mean vibration acceleration of branches: (a) the mean acceleration of B₁₂ and (b) the mean acceleration of B₂₁.

In Figure 6, it is evident that when the frequency of the excitation force remains constant, the average vibration acceleration a_v of the branch exhibits a non-linear trend of linear increase with the rise in phase angle. At different frequencies, the vibration acceleration of each branch shows significant variations with the increase in phase angle. Simultaneously, under the same excitation parameters, the amplitude of vibration acceleration differs among various branches.

4. Discussion

4.1. Analysis of Vibration Difference of Branches

In the current research on fruit vibration harvesting, objective differences in the vibration acceleration of branches exist. However, the underlying reasons for these differences remain unexplained [21–24]. To analyze the differences in vibration accelerations between branches B₁₂ and B₂₁ shown in Figures 4 and 5, a branch vibration model was constructed using the concentrated mass method as depicted in Figure 7. The vibration harvest system was divided into primary branches, secondary branches, trunk, and exciter. Branches were labeled as B₁, B₁₁, B₁₂, B₂, B₂₁, B₂₂, as illustrated in Figure 7a. By simplifying the other branches and leaves into concentrated masses, vibration models for branches B₁₂ and B₂₁ were derived, as shown in Figure 7b,c. Through force balance relationships, vibration differential equations for B₁₂ and B₂₁ were established (Equations (4) and (5)). The results indicate that the mass and position of other branches related to a specific branch influence its vibration characteristics, leading to varied vibration accelerations among different branches. This underscores the need for multiple excitation frequencies to enhance fruit harvest efficiency in fruit trees.

$$EI \frac{\partial^4 y}{\partial x^4} + \left(\begin{matrix} \rho A(x) + M\delta(x-l) + M_2\delta(x-l_2) + m_3\delta(x-l_3) + \\ m_{11}\delta(x-l_{11}) + m_{12}\delta(x-l_{12}) \end{matrix} \right) \ddot{y} = \delta(x-l)F(\omega, \varphi, t) \quad (4)$$

$$EI \frac{\partial^4 y}{\partial x^4} + \left(\begin{matrix} \rho A(x) + M\delta(x-l) + M_1\delta(x-l_1) \\ +m_3\delta(x-l_3) + m_{22}\delta(x-l_{22}) + m_{21}\delta(x-l_{21}) \end{matrix} \right) \ddot{y} = \delta(x-l)F(\omega, \varphi, t) \quad (5)$$

In the equation, E denotes the elastic modulus of the fruit tree, while I represents the moment of inertia of the trunk section. ρ stands for the density of the beam, $A(x)$ signifies the cross-sectional area of the trunk, and δ represents the distribution function of the concentrated mass. y indicates the direction of change in the vibration displacement of the trunk or branches.

The branch vibration can be regarded as beam vibration. The vibration transfer function $H(\omega)$ of the branch is expressed by superimposing multiple modes in Equation (6).

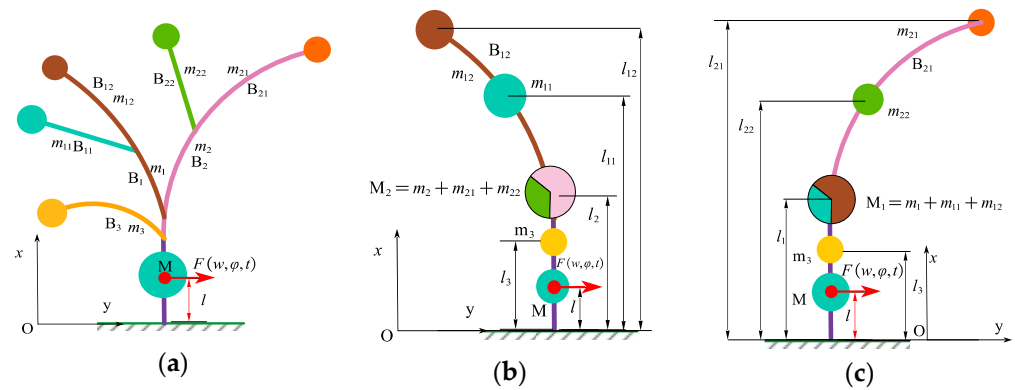


Figure 7. Vibration modeling of branches: (a) simplification of the structure of fruit trees; (b) simplified model of tree B₁₂; and (c) simplified model of branch B₂₁.

$$H(\omega) = \sum_{r=1}^N \frac{1}{m_r} \frac{\{\varphi_r\}\{\varphi_r\}^T}{\omega_r^2 - \omega^2 + j\xi_r\omega_r\omega} = \frac{y(\omega)}{F(\omega, \varphi, t)} \quad (6)$$

where $y(\omega)$ represents the vibration displacement of the branch, and $F(\omega, \varphi, t)$ represents the exciting force generated by DSEE. ω_r is the r th-order vibration mode frequency of the branch, ω is the excitation frequency, j is the unit complex number, $j^2 = -1$, and ξ_r is the damping of the r th-order mode. $\{\varphi_r\}$ is the mode function of r -th mode; m_r is the modal mass.

From the vibration transfer function of tree branches, it is evident that when the spatial structure of the branches and the excitation frequency of the fruit tree remain constant, the vibration transfer function of the fruit tree is determined. Increasing the amplitude F of the excitation force by the phase angle φ results in a larger displacement of branch vibration and a larger acceleration value. This explains why the test results in Figures 5 and 6 align with the vibration transfer function $H(\omega)$ of the branches. This also validates why the vibration acceleration of branches can increase with the growing phase angle φ of the excitation force.

4.2. Significance of Amplitude Regulation of Excitation Force

During trunk vibration harvesting, the vibration acceleration of fruits primarily relies on the exciting force generated by the shaker [25–27]. Nevertheless, the amplitude and frequency of the excitation force generated by current exciters follow a square relation. Optimal exciting frequencies for fruit vibration harvesting vary among different types of fruit trees [7,9,23]. When the excitation force amplitude is small, it can lead to a low fruit detachment rate due to insufficient force. Conversely, a large excitation force amplitude may cause excessive vibration acceleration, surpassing the required force for fruit separation from the stem. Additionally, high excitation force amplitudes can potentially damage the fruit trees [24]. The DSEE addresses the issue of un-adjustable excitation force amplitudes at a constant frequency. By increasing the vibration force amplitude at a lower excitation frequency, the vibration acceleration of branches can be enhanced, leading to a higher fruit detachment rate. Conversely, decreasing the vibration force amplitude at a higher exciting frequency can mitigate the risk of excessive force that could potentially damage the fruit trees.

4.3. Future Research Plans

The vibration characteristics of fruit trees vary significantly due to differences in tree shapes. The DSEE developed in this study enables the independent adjustment of excitation force amplitude and frequency. However, each fruit tree possesses unique spatial structures influenced by growth, pruning, and other factors, resulting in changing spectral properties over the years. Previous research primarily relied on experimental methods

to measure vibration modes of fruit trees, making it challenging to directly apply these results in selecting excitation parameters for next year's fruit tree vibration harvest. Rapidly perceiving the vibration characteristics of fruit trees has thus become a complex task.

To effectively select the optimal exciting frequency for fruit tree vibration harvesting, it is crucial to first obtain the vibration characteristics of the specific fruit tree. This allows for adjusting the excitation force amplitude through the phase Angle φ of the DSEE. By coupling excitation force parameters with the unique vibration characteristics of fruit trees, intelligent vibration harvesting can be achieved. Therefore, our study aims to explore efficient modal frequency detection for fruit trees during the vibration harvesting process. Utilizing modal frequency as the input signal, a control algorithm for adjusting the exciting force parameters of fruit tree vibration harvesting will be developed, enabling intelligent vibration harvesting of fruit trees.

5. Conclusions

The DSEE developed is composed of two sets of symmetrical eccentric blocks, and it has the capability to adjust the excitation force amplitude through its phase angle. When maintaining a constant excitation frequency, increasing the phase angle φ of the DSEE results in an amplification of the exciting force amplitude, subsequently leading to higher vibration accelerations of the branches. Conversely, reducing the phase angle φ tends to decrease the branch vibration acceleration.

Furthermore, theoretical analysis in the discussion reveals that the average vibration acceleration values vary among different branches under the same excitation parameters due to differences in equivalent concentrated mass size and distribution positions across branches.

Author Contributions: H.J. and L.W. designed the experiment. J.L., A.T. and Y.L. worked on data collection. H.J. and C.M. carried out the experiments, analyzed the data, and wrote the original manuscript with the help and the constructive criticism of C.L. All authors have read and agreed to the published version of the manuscript.

Funding: This research was funded by the National Natural Science Foundation of China [grant number: 52265036] and Department of Science and Technology, Xinjiang Uygur Autonomous Region [grant number: 2022B02028-3].

Data Availability Statement: All data have been presented in the paper, Figures 4 and 5.

Conflicts of Interest: All authors declare no conflicts of interest. We identify and declare that there are no personal circumstances or interests that may be perceived as inappropriately influencing the representation or interpretation of the reported research results.

References

1. Atanasov, A.G.; Sabharanjak, S.M.; Zengin, G.; Mollica, A.; Szostak, A.; Simirgiotis, M.; Huminiecki, L.; Horbanczuk, O.K.; Nabavi, S.M.; Mocan, A. Pecan nuts: A review of reported bioactivities and health effects. *Trends Food Sci. Technol.* **2018**, *71*, 246–257. [[CrossRef](#)]
2. Kumari, S.; Seth, A.; Sharma, S.; Attri, C. A holistic overview of different species of *Potentilla* a medicinally important plant along with their pharmaceutical significance: A review. *J. Herb. Med.* **2021**, *29*, 100460. [[CrossRef](#)]
3. Salas-Salvadó, J.; Casas-Agustench, P.; Salas-Huetos, A. Cultural and historical aspects of Mediterranean nuts with emphasis on their attributed healthy and nutritional properties. *Nutr. Metab. Cardiovas.* **2011**, *21*, S1–S6. [[CrossRef](#)] [[PubMed](#)]
4. Machado, A.P.D.; do Nascimento, R.D.; Alves, M.D.; Reguengo, L.M.; Junior, M.R.M. Brazilian tucuma-do-Amazonas and tucuma-do-Para fruits: Bioactive composition, health benefits, and technological potential. *Food Res. Int.* **2022**, *151*, 110902. [[CrossRef](#)] [[PubMed](#)]
5. Du, X.; Chen, K.; Ma, Z.; Wu, C.; Zhang, G. Design, Construction, and Evaluation of a Three-Dimensional Vibratory Harvester for Tree Fruit. *Appl. Eng. Agric.* **2020**, *36*, 221–231. [[CrossRef](#)]
6. Du, X.Q.; Chen, D.; Zhang, Q.; Scharf, P.A.; Whiting, M.D. Dynamic responses of sweet cherry trees under vibratory excitations. *Biosyst. Eng.* **2012**, *111*, 305–314. [[CrossRef](#)]
7. Du, X.Q.; Jiang, F.; Li, S.T.; Xu, N.N.; Li, D.W.; Wu, C.Y. Design and experiment of vibratory harvesting mechanism for Chinese hickory nuts based on orthogonal eccentric masses. *Comput. Electron. Agric.* **2019**, *156*, 178–186. [[CrossRef](#)]

8. Cetinkaya, C.; Polat, R.; Ozalp, A.F. Investigation of the vibration effect of using single or double eccentric mass in the trunk shakers used in fruit harvesting. *Eng. Sci. Technol.* **2022**, *35*, 101228. [[CrossRef](#)]
9. Cao, J.L.; Bai, X.P.; Xu, D.C.; Li, W.B.; Chen, C.C. Experiment and analysis on walnut (*Juglans regia* L.) Shedding force based on low-frequency vibration response. *Ind. Crop. Prod.* **2023**, *204*, 117242. [[CrossRef](#)]
10. Lang, Z. A fruit tree stability model for static and dynamic loading. *Biosyst. Eng.* **2003**, *85*, 461–466. [[CrossRef](#)]
11. Lang, Z. Dynamic modelling structure of a fruit tree for inertial shaker system design. *Biosyst. Eng.* **2006**, *93*, 35–44. [[CrossRef](#)]
12. Wei, J.; Yang, G.Y.; Yan, H.; Jing, B.B.; Yu, Y. Rigid-flexible coupling simulation and experimental vibration analysis of pistachio tree for optimal mechanized harvesting efficiency. *Mech. Adv. Mater. Struc.* **2021**, *28*, 2360–2369. [[CrossRef](#)]
13. Castro-Garcia, S.; Aragon-Rodriguez, F.; Arias-Calderon, R.; Sola-Guirado, R.R.; Gil-Ribes, J.A. The contribution of fruit and leaves to the dynamic response of secondary branches of orange trees. *Biosyst. Eng.* **2020**, *193*, 149–156. [[CrossRef](#)]
14. Yang, Y.B.; Yang, Y.T.; Su, H.H. Behavior of the tree branches, trunk, and root anchorage by nonlinear finite element analysis. *Adv. Struct. Eng.* **2005**, *8*, 1–14. [[CrossRef](#)]
15. Liu, T.H.; Luo, G.; Ehsani, R.; Toudeshki, M.; Zou, X.J.; Wang, H.J. Simulation study on the effects of tine-shaking frequency and penetrating depth on fruit detachment for citrus canopy-shaker harvesting. *Comput. Electron. Agric.* **2018**, *148*, 54–62. [[CrossRef](#)]
16. Zhou, J.; Xu, L.Y.; Zhao, J.W.; Hang, X.C.; Zhou, H.P. Effective excitation conditions for the intense motion of the ginkgo seed-stem system during mechanical vibration harvesting. *Biosyst. Eng.* **2022**, *215*, 239–248. [[CrossRef](#)]
17. Coelho, A.L.D.; Santos, F.L.; Pinto, F.D.D.; de Queiroz, D.M. Dynamic test for determining the elastic modulus of coffee fruit-stem-branch system. *Acta Sci.-Technol.* **2017**, *39*, 579–586. [[CrossRef](#)]
18. Wang, Y.F.; Wang, W.Z.; Fu, H.; Yang, Z.; Lu, H.Z. Detachment patterns and impact characteristics of litchi fruit during vibrational harvesting. *Sci. Hortic.* **2022**, *295*, 110836. [[CrossRef](#)]
19. He, L.; Zhou, J.F.; Du, X.Q.; Chen, D.; Zhang, Q.; Karkee, M. Energy efficacy analysis of a mechanical shaker in sweet cherry harvesting. *Biosyst. Eng.* **2013**, *116*, 309–315. [[CrossRef](#)]
20. He, L.; Liu, X.; Du, X.; Wu, C. In-situ identification of shaking frequency for adaptive vibratory fruit harvesting. *Comput. Electron. Agric.* **2020**, *170*, 105245. [[CrossRef](#)]
21. Niu, Z.J.; Xu, Z.; Deng, J.T.; Zhang, J.; Pan, S.J.; Mu, H.T. Optimal vibration parameters for olive harvesting from finite element analysis and vibration tests. *Biosyst. Eng.* **2022**, *215*, 228–238. [[CrossRef](#)]
22. Lin, H.; Sun, L.H. Vibration responses characteristics of a Ginkgo biloba tree excited under harmonic excitation. *PLoS ONE* **2021**, *16*, e0256492. [[CrossRef](#)] [[PubMed](#)]
23. Xuan, Y.; Xu, L.Y.; Liu, G.H.; Zhou, J. The Potential Influence of Tree Crown Structure on the Ginkgo Harvest. *Forests* **2021**, *12*, 366. [[CrossRef](#)]
24. Pezzi, F.; Caprara, C. Mechanical grape harvesting: Investigation of the transmission of vibrations. *Biosyst. Eng.* **2009**, *103*, 281–286. [[CrossRef](#)]
25. Kazama, E.H.; da Silva, R.P.; Tavares, T.D.; Correa, L.N.; Estevam, F.N.D.; Nicolau, F.E.D.; Maldonado, W. Methodology for selective coffee harvesting in management zones of yield and maturation. *Precis. Agric.* **2021**, *22*, 711–733. [[CrossRef](#)]
26. Homayouni, T.; Gholami, A.; Toudeshki, A.; Afsah-Hejri, L.; Ehsani, R. Estimation of proper shaking parameters for pistachio trees based on their trunk size. *Biosyst. Eng.* **2022**, *216*, 121–131. [[CrossRef](#)]
27. Zhou, J.F.; He, L.; Karkee, M.; Zhang, Q. Analysis of shaking-induced cherry fruit motion and damage. *Biosyst. Eng.* **2016**, *144*, 105–114. [[CrossRef](#)]

Disclaimer/Publisher’s Note: The statements, opinions and data contained in all publications are solely those of the individual author(s) and contributor(s) and not of MDPI and/or the editor(s). MDPI and/or the editor(s) disclaim responsibility for any injury to people or property resulting from any ideas, methods, instructions or products referred to in the content.